

Supplemental Online Content

Yilmaz K, Goletz S, Pas HH, et al. Clinical and serological characterization of orf-induced immunobullous disease. *JAMA Dermatol*. Published online March 30, 2022.
doi:10.1001/jamadermatol.2022.0290

eMethods.

eDiscussion.

eFigure 1. Serological diagnosis of orf-induced anti-laminin 332 pemphigoid of the index patient (Case 1)

eFigure 2. Immunoblot analysis of orf-induced (bullous) pemphigoid

eFigure 3. IgG1 reactivity against laminin 332 by IF microscopy using Biochip™ mosaic

eFigure 4. Detection of IgG3 autoantibodies against laminin 332 by IF microscopy using Biochip™ mosaic

eFigure 5. Positive and negative controls for IgG3 reactivity against laminin 332 by IF microscopy using Biochip™ mosaic

eFigure 6. Analysis of IgG subclass-specific autoantibodies against laminin 332 of the index patient (Case 1) using Biochip™ mosaic

eTable. Clinical and immunological aspects of the 7 other hitherto published cases of orf-induced pemphigoid

eReferences.

This supplemental material has been provided by the authors to give readers additional information about their work.

eMethods

Indirect Immunofluorescence

For the detection of serum anti-laminin 332 reactivity a recently developed indirect IF test based on the recombinant expression of the α 3, β 3, and γ 2 chains of laminin 332 and the recombinant laminin 332 heterotrimer on the cell surface of a human cell line (HEK293) was used as described previously (Euroimmun, Lübeck, Germany)¹⁻². In brief, all sera were subjected to the indirect IF biochip mosaic with six different substrates comprising HEK293 cells transfected with pTriEx-1 constructs for (i) LAMA3, (ii) LAMB3 (+/- His tag), (iii) LAMC2 (+/- His-tag) (encoding for the α 3, β 3, and γ 2 chains, respectively), (iv, v) co-transfected all three plasmids encoding for the heterotrimer (+/- His tag), and (vi) the empty plasmid, as described recently¹. All sera were applied in a 1:10 dilution in PBS supplemented with 0.2 % tween-20, and, after washing, bound autoantibodies were detected by FITC-labelled mouse IgG subclass-specific detection antibodies (IgG1, clone 8c/6-39, dilution 1:100; IgG2, clone HP-6014, dilution 1:50; IgG3, HP-6050, dilution 1:100; IgG4, clone HP-6025, dilution 1:100; all Sigma-Aldrich, St. Louis, MO, USA). Pictures were taken using a Bioevo Keyence BZ-9000 fluorescence microscope (Keyence Deutschland GmbH, Neu-Isenburg, Germany).

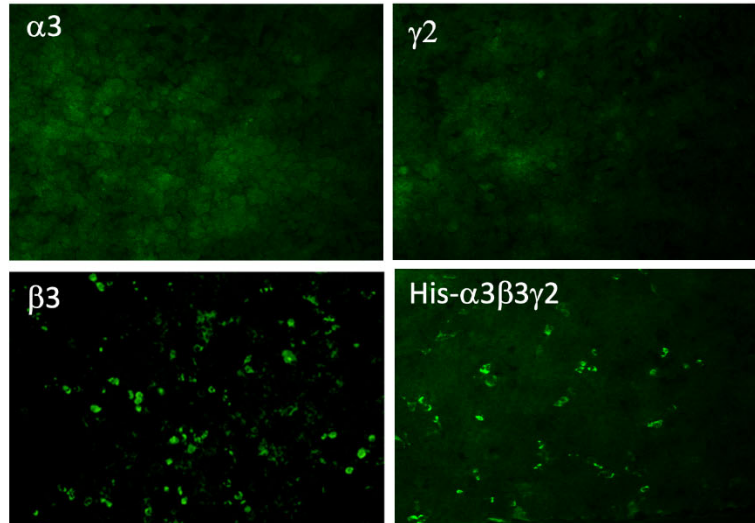
Immunoblotting

Immunoblotting was performed with (i) extract of human dermis (for reactivity against p200 protein and full-length type VII collagen), (ii) recombinant non-collagenous (NC1) domain of type VII collagen, and (iii) extracellular matrix of cultured human keratinocytes (for reactivity against laminin 332) as previously reported³⁻⁵. As secondary antibodies horseradish peroxidase-conjugated sheep anti-IgG1 and IgG3 antibodies were applied (Binding Site, Birmingham, UK).

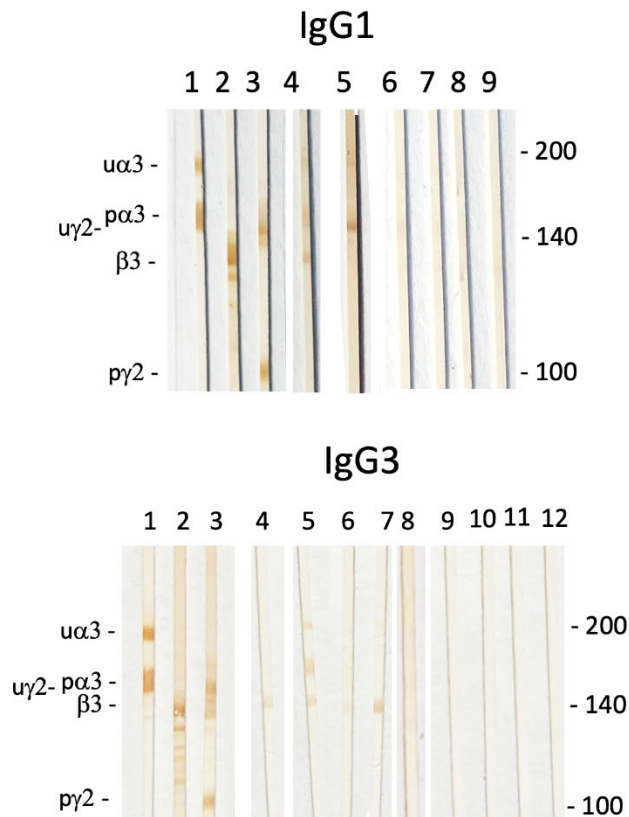
eDiscussion

The relationship between viral infections and the induction of autoimmunity has been much disputed. In this context, Blaszek *et al.* found high frequencies of Torque Teno virus (TTV) in sera of bullous pemphigoid (BP) patients as well as significant *in silico* similarity of BP180 and the virus proteins in conjunction with a cellular response to TTV-specific sequences in TTV-positive BP patients⁶. By contrast, in Case 4 (Table 1) no overlap larger than four consecutive amino acids could be detected in a protein-protein blast of four orf strains against all transcripts of laminin 332⁷. This can be attributed to a conformational epitope, as the authors correctly pointed out⁷. As previously proposed, an alternative explanation may be the alteration or unmasking of laminin 332 by orf, leading to an increased immunogenicity in predisposed individuals⁷⁻⁹. This hypothesis is in line with the explanation for solid laminin 332-expressing tumors as trigger for anti-laminin 332 MMP that is associated with malignancies in 25-30% of patients^{1,10}.

eFigure 1. Serological diagnosis of orf-induced anti-laminin 332 pemphigoid of the index patient (Case 1). Indirect immunofluorescence microscopy using membrane-bound recombinant laminin $\alpha 3$, $\beta 3$, $\gamma 2$, and the heterotrimer with His-tag expressed on HEK293 cells (His- $\alpha 3\beta 3\gamma 2$), respectively. IgG3 autoantibodies against the laminin 332 $\beta 3$ chain (left lower panel) and the heterotrimer (right lower panel) are seen.

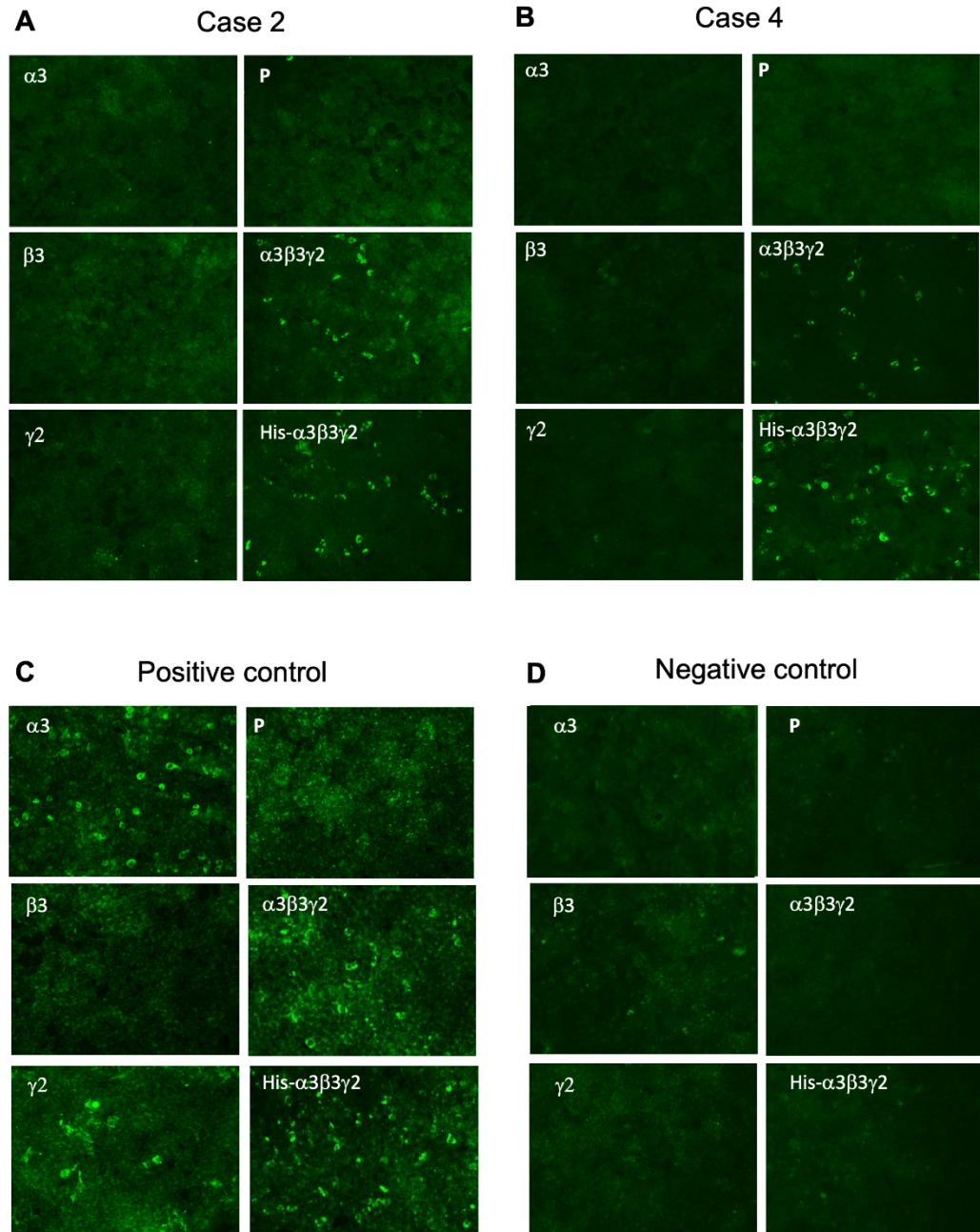


eFigure 2. Immunoblot analysis of orf-induced (bullous) pemphigoid. Representative pictures of anti-laminin 332 IgG1 (upper panel) and IgG3 reactivity (lower panel) by immunoblotting with extracts of extracellular matrix of cultured keratinocytes. **Upper panel:** Case 1 recognized the $\beta 3$ and weakly the $p\alpha 3$ chain (lane 4) and Case 2 the $u\gamma 2$ chain (lane 5). Commercial antibodies against the unprocessed ($u\alpha 3$) and processed $\alpha 3$ ($p\alpha 3$; lane 1), $\beta 3$ (lane 2) as well as $u\gamma 2$ and $p\gamma 2$ chains (lane 3) served as positive controls. Sera of healthy blood donors are shown in lanes 6-9. **Lower panel:** Cases 1-4 (lanes 4-7) showed IgG3 reactivity with the $\beta 3$ chain and Case 2 additional reactivity with $u\alpha 3$ and $p\alpha 3$ (lane 5). Case 5 revealed no IgG3 reactivity (lane 8). Commercial antibodies against the unprocessed ($u\alpha 3$) and processed $\alpha 3$ ($p\alpha 3$; lane 1), $\beta 3$ (lane 2) as well as $u\gamma 2$ and $p\gamma 2$ chains (lane 3) served as positive controls. Sera of healthy blood donors are shown in lanes 9-12. Numbers to the right indicate molecular weight markers in kDa.



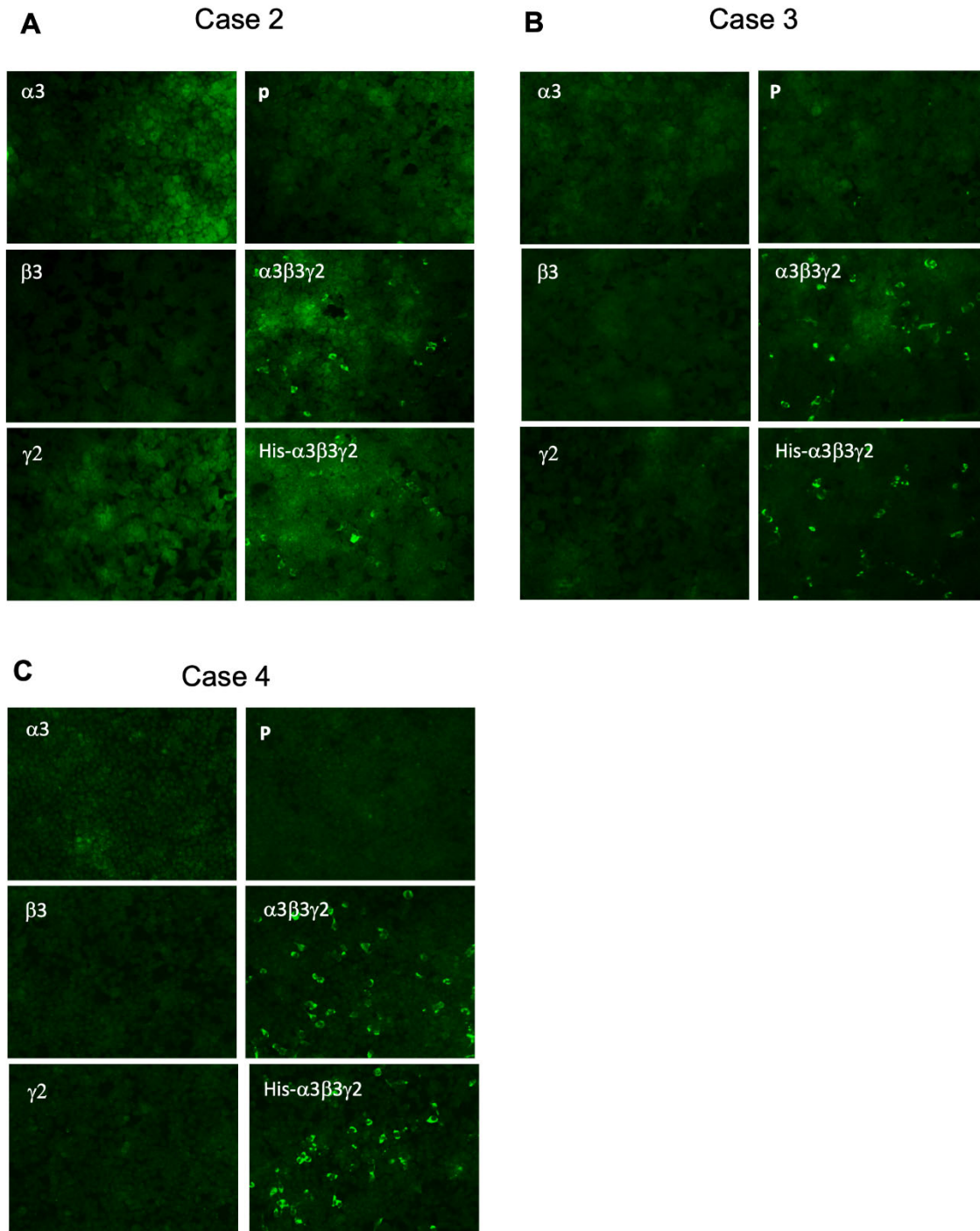
eFigure 3. IgG1 reactivity against laminin 332 by IF microscopy using Biochip™ mosaic. Detection of IgG1 autoantibodies against laminin 332 heterotrimer $\alpha 3\beta 3\gamma 2$ (-/+ His-tag) was shown for Case 2 (A) and Case 4 (B). All other fields were negative. C: Serum of a patient with anti-laminin 332 mucous membrane pemphigoid (MMP) was used as a positive control. IgG1 reactivity against $\alpha 3$, $\gamma 2$ subunits as well as the heterotrimer $\alpha 3\beta 3\gamma 2$ (-/+ His-tag) was seen. D: Serum of a healthy blood donor was used as a negative control. Serum dilution at 1:10 in PBS-T. Anti-IgG1 FITC antibody was diluted at 1:100 in PBS-T. P, empty plasmid.

IgG1 FITC



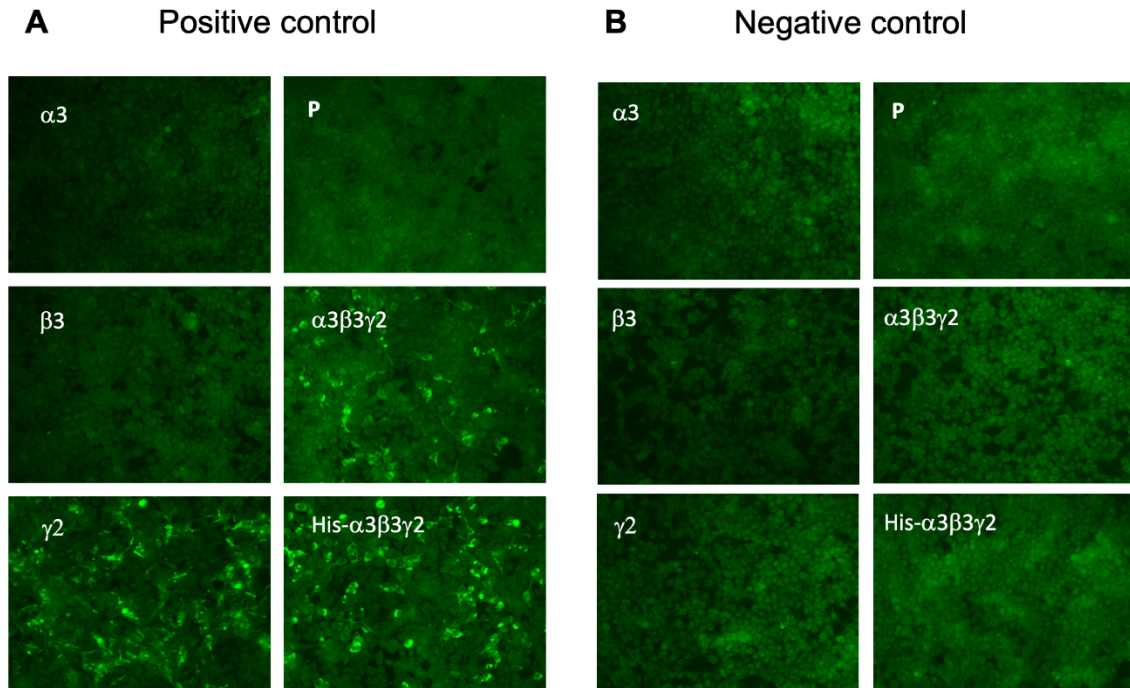
eFigure 4. Detection of IgG3 autoantibodies against laminin 332 by IF microscopy using Biochip™ mosaic. IgG3 autoantibodies against laminin 332 trimer $\alpha3\beta3\gamma2$ (-/+ His-tag) were detected in Case 2 (A), Case 3 (B) and Case 4 (C). In contrast, no reactivity with the single chains of laminin 332 was detected. Serum dilution at 1:10 in PBS-T. Anti-IgG3 FITC antibody was diluted at 1:100 in PBS-T. P, empty plasmid.

IgG3 FITC



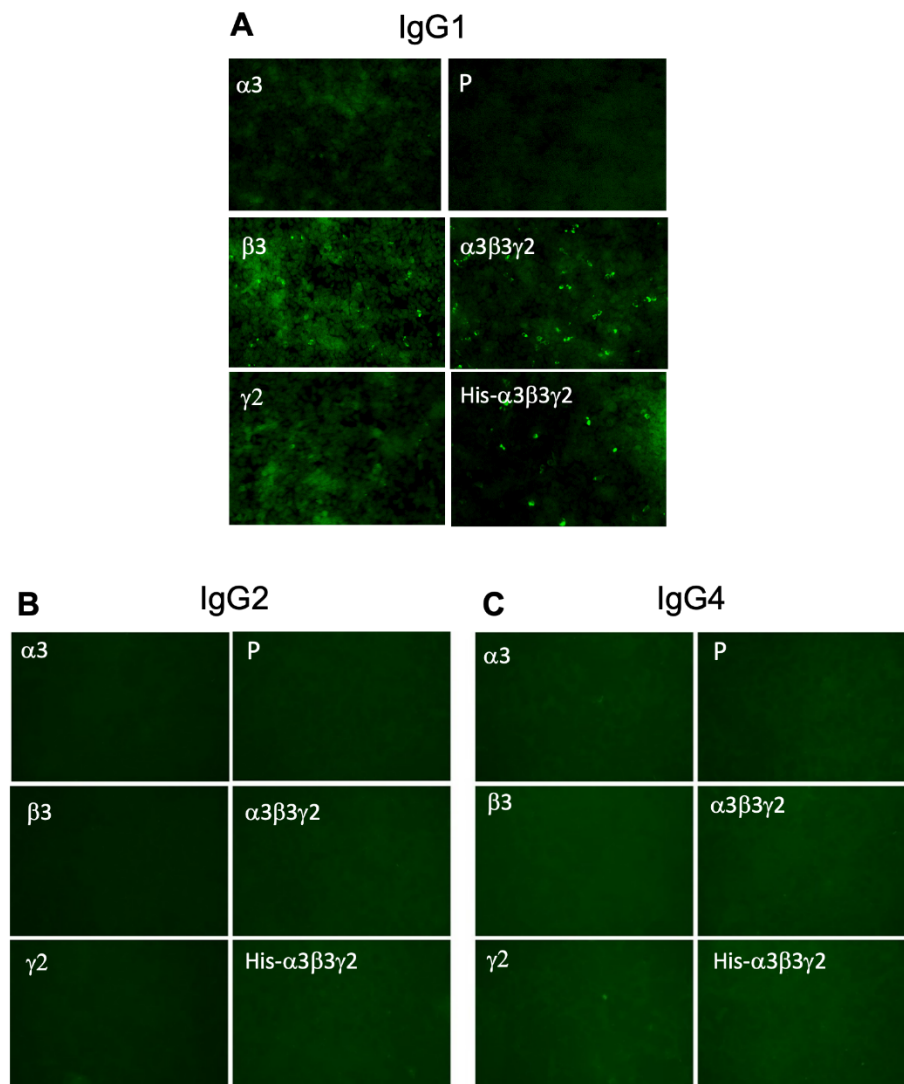
eFigure 5. Positive and negative controls for IgG3 reactivity against laminin 332 by IF microscopy using Biochip™ mosaic. **A:** Serum of a patient with anti-laminin 332 MMP was used as positive control and revealed IgG3 autoantibodies against $\gamma 2$ subunit of laminin 332 and the heterotrimer $\alpha 3\beta 3\gamma 2$ (-/+ His-tag). **B:** Negative results of a healthy blood donor were shown. Serum dilution at 1:10 in PBS-T. Anti-IgG3 FITC antibody was diluted at 1:100 in PBS-T. P, empty plasmid.

IgG3 FITC



eFigure 6. Analysis of IgG subclass-specific autoantibodies against laminin 332 of the index patient (Case 1) using Biochip™ mosaic. **A:** Serum of the index patient revealed IgG1 autoantibodies against laminin 332 heterotrimer $\alpha3\beta3\gamma2$ (-/+ His-tag) and $\beta3$ chain, whereas no reactivity with $\alpha3$ and $\gamma2$ chain was seen. Furthermore, no IgG2 (**B**) and IgG4 (**C**) autoantibodies could be detected. IgG3 reactivity was detailed separately in eFigure 1. Serum was diluted at 1:10 and secondary antibodies at 1:100 (IgG2, 1:50) in PBS-T. P, empty plasmid.

Case 1



eTable. Clinical and immunological aspects of the 7 other hitherto published cases of orf-induced pemphigoid

Case #	Age	Sex	Interval between orf and blister formation	Direct IF BMZ	Indirect IF on Salt-split skin	ELISA/ Immunoblot	Clinical features		Reference
							Skin	Mucous membranes	
Predominant skin lesions									
6	62	f	3-4 weeks	C3	negative	not performed	++	-	9
7	37	m	3 weeks	C3	negative	not performed	++	-	9
8	n/a	n/a	2-3 weeks	C3	negative	not performed	++	-	9
9	n/a	n/a	2-3 weeks	C3	negative	not performed	++	-	9
10	n/a	n/a	2-3 weeks	C3	negative	not performed	++	-	9
11	51	f	16 days	IgG, C3	not performed	not performed	++	+ oral	11
12	42	f	4 weeks	IgG, C3	IgG1, IgG3, dermal side	Type VII collagen ELISA ^a , 38 U/ml, cut-off < 20; laminin 332 Biochip™ and IB extracellular matrix, negative ^b	++	+ oral, nasal	12
Predominant mucosal lesions									
13	55	m	several weeks	IgG, IgM, IgA, C3 (n-serrated)	negative	all negative	+	++ oral, nasal, ocular	13

^a Euroimmun, Lübeck, Germany; ^b data not shown

BMZ, basement membrane zone; IF, indirect immunofluorescence; n/a, not available

eReferences

1. Goletz S, Probst C, Komorowski L, et al. A sensitive and specific assay for the serological diagnosis of antilaminin 332 mucous membrane pemphigoid. *Br J Dermatol*. 2019;180(1):149-156.
2. Goletz S, Giurdanella F, Holtsche MM, et al. Comparison of Two Diagnostic Assays for Anti-Laminin 332 Mucous Membrane Pemphigoid. *Front Immunol*. 2021;12:773720.
3. Holtsche MM, Goletz S, von Georg A, et al. Serologic characterization of anti-p200 pemphigoid: Epitope spreading as a common phenomenon. *J Am Acad Dermatol*. 2021;84(4):1155-1157.
4. Lau I, Goletz S, Holtsche MM, Zillikens D, Fechner K, Schmidt E. Anti-p200 pemphigoid is the most common pemphigoid disease with serum antibodies against the dermal side by indirect immunofluorescence microscopy on human salt-split skin. *J Am Acad Dermatol*. 2019;81(5):1195-1197.
5. van Beek N, Kruger S, Fuhrmann T, et al. Multicenter prospective study on multivariant diagnostics of autoimmune bullous dermatoses using the BIOCHIP(TM) technology. *J Am Acad Dermatol*. 2020.
6. Blazsek A, Sillo P, Ishii N, et al. Searching for foreign antigens as possible triggering factors of autoimmunity: Torque Teno virus DNA prevalence is elevated in sera of patients with bullous pemphigoid. *Exp Dermatol*. 2008;17(5):446-454.
7. van den Bos RR, Middelburg T, van Biezen P, van der Eijk AA, Pas HH, Diercks GF. Orf-induced pemphigoid with antilaminin-332 antibodies. *Br J Dermatol*. 2012;167(4):956-958.
8. White KP, Zedek DC, White WL, et al. Orf-induced immunobullous disease: A distinct autoimmune blistering disorder. *J Am Acad Dermatol*. 2008;58(1):49-55.
9. Murphy JK, Ralfs IG. Bullous pemphigoid complicating human orf. *Br J Dermatol*. 1996;134(5):929-930.
10. Egan CA, Lazarova Z, Darling TN, Yee C, Coté T, Yancey KB. Anti-epiligrin cicatricial pemphigoid and relative risk for cancer. *Lancet*. 2001;357(9271):1850-1851.
11. Macfarlane AW. Human orf complicated by bullous pemphigoid. *Br J Dermatol*. 1997;137(4):656-657.
12. Daneshpazhooh M, Mahmoudi H, Toosi R, Tavakolpour S, Schmidt E, Zillikens D. Post-orf epidermolysis bullosa acquisita. *J Eur Acad Dermatol Venereol*. 2019;33(3):e118-e119.
13. van Lingen RG, Frank RG, Koopman RJ, Jonkman MF. Human orf complicated by mucous membrane pemphigoid. *Clin Exp Dermatol*. 2006;31(5):711-712.